

A Novel Broadband Channel Estimation Technique Based on Dual-Module QGAN

Li Ting^{1*} and Zhang Jinbiao¹

¹ School of Communications and Information Engineering
Nanjing University of Posts and Telecommunications, Nanjing, Jiangsu, 210000, China
[e-mail: lit@njupt.edu.cn]

*Corresponding author: Li Ting

*Received October 6, 2023; revised March 19, 2024; accepted April 20, 2024;
published May 31, 2024*

Abstract

In the era of 6G, the rapid increase in communication data volume poses higher demands on traditional channel estimation techniques and those based on deep learning, especially when processing large-scale data as their computational load and real-time performance often fail to meet practical requirements. To overcome this bottleneck, this paper introduces quantum computing techniques, exploring for the first time the application of Quantum Generative Adversarial Networks (QGAN) to broadband channel estimation challenges. Although generative adversarial technology has been applied to channel estimation, obtaining instantaneous channel information remains a significant challenge. To address the issue of instantaneous channel estimation, this paper proposes an innovative QGAN with a dual-module design in the generator. The adversarial loss function and the Mean Squared Error (MSE) loss function are separately applied for the parameter updates of these two modules, facilitating the learning of statistical channel information and the generation of instantaneous channel details. Experimental results demonstrate the efficiency and accuracy of the proposed dual-module QGAN technique in channel estimation on the PennyLane quantum computing simulation platform. This research opens a new direction for physical layer techniques in wireless communication and offers expanded possibilities for the future development of wireless communication technologies.

Keywords: Channel Estimation, Instantaneous Channel, Quantum Generative Adversarial Networks, MSE Optimization

1. Introduction

With the rapid development and promotion of 5G and 6G communication technologies [1,2], the world is entering a prosperous era of communication technology. Since Claude Shannon proposed the theory of information in 1948 [3], the field of communication has undergone several technological innovations, and the emergence of 5G and 6G signifies a leap in communication speed [4]. These technologies have become the core infrastructure supporting cutting-edge technologies such as the Internet of Things (IoT), Augmented Reality (AR), Virtual Reality (VR), and autonomous driving [5]. However, this rapid progress also brings unprecedented technical challenges, especially in the critical technical field of accurately estimating and adapting to complex channel environments [6,7].

Traditional channel estimation methods, such as the Least Squares (LS) and Minimum Mean Square Error (LMMSE), have achieved certain success in early communication technologies [8]. However, when facing complex and variable channel environments, these methods often fail to meet the requirements of high precision and low complexity [9]. In recent years, the application of machine learning technology, especially Generative Adversarial Networks (GAN), in channel estimation has attracted widespread attention [10]. These methods can accurately simulate complex data distributions by learning the statistical properties of channels, providing a new perspective for the estimation of complex channel environments [11,12,13]. However, traditional machine learning methods still face constraints in computational load and real-time performance when dealing with large-scale data and high-dimensional problems [14,15]. The rise of quantum computing technology brings new possibilities to machine learning [16,17]. Quantum machine learning, utilizing the high parallelism and modeling capabilities of quantum computing, shows potential for higher efficiency and precision in specific tasks compared to classical machine learning [18,19]. In particular, the proposal of Quantum Generative Adversarial Networks (QGAN) provides a new solution for the problem of channel estimation [20].

This paper aims at the problem of estimating large-scale instantaneous channels in 6G and designs a Quantum Generative Adversarial Network with a dual-module network structure. On one hand, by utilizing quantum computing technology, it can break through the computational bottleneck of large-scale channel estimation. On the other hand, by applying the adversarial loss function and the MSE loss function to the two modules separately, it can solve the limitation that the generative adversarial model can only obtain channel statistical properties and the problem of poor generalization performance of the generator optimized only by the MSE loss function. The proposed Quantum Generative Adversarial Network is essentially a quantum-classical hybrid network, implemented with parameterized quantum circuits, capable of running on real quantum computers, while training is performed using classical optimization algorithms on classical computers.

2. GAN-Based OFDM Channel Estimation

2.1 OFDM System and Interpolated Channel Estimation

The architecture of the OFDM system is shown in Fig. 1:

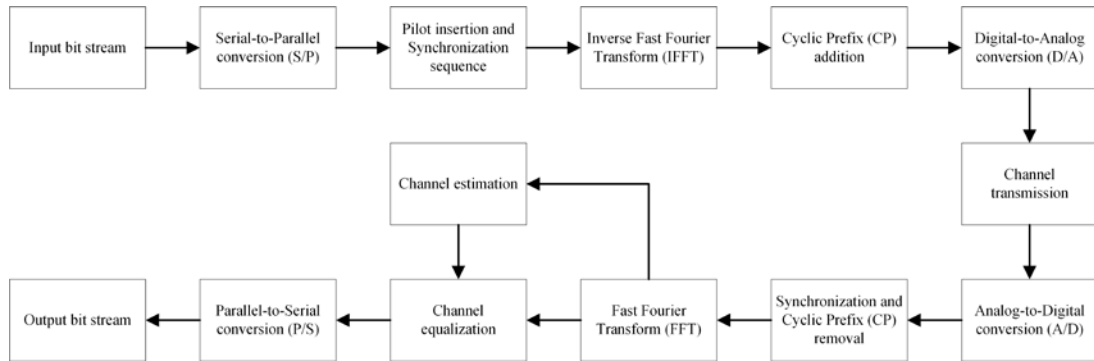


Fig. 1. OFDM system architecture

Within the OFDM transmission architecture, consider a frame structure composed of N_t OFDM symbols. Each symbol is composed of N_s sub-carriers. In this structure, the index range of symbols is defined as $n \in [0, N_t - 1]$ and the index range of sub-carriers is defined as $m \in [0, N_s - 1]$. After removing the cyclic prefix (CP), its received signal model can be represented by the following equation:

$$Y_{m,n} = H_{m,n} X_{m,n} + W_{m,n} \quad (1)$$

Where $X_{m,n}$ is the transmitted signal, $H_{m,n}$ represents the channel frequency response (CFR), and $W_{m,n}$ is the additive noise.

The accuracy of channel estimation largely determines the performance of the OFDM system. In traditional pilot-based channel estimation strategies, known pilot signals are inserted into the OFDM frame. At the receiver, these pilot signals are first used to estimate the channel frequency response (CFR), then interpolation techniques are employed to estimate over data sub-carriers, thereby achieving CFR estimation across the entire OFDM symbol.

Specifically, the interpolation method for channel estimation is based on known CFRs over the pilots to estimate the CFR across the entire OFDM symbol. Once the channel responses on certain sub-carriers are obtained, interpolation techniques can be employed to estimate the channel response on other sub-carriers. Common interpolation methods include linear interpolation, polynomial interpolation, and spline interpolation [21].

For instance, for linear interpolation, if we know the channel responses on sub-carriers k and $k + 1$ as H_k and H_{k+1} respectively, then the channel response on any sub-carrier i between k and $k + 1$ can be estimated as:

$$H_i = H_k + \frac{i-k}{k+1-k} \times (H_{k+1} - H_k) \quad (2)$$

For polynomial interpolation, a polynomial is used to fit known data points, and this polynomial is then used to estimate the values of unknown points. For example, in quadratic polynomial interpolation, let the estimated channel response on subcarrier i be H_i , and the known channel responses on subcarriers k , $k + 1$, and $k + 2$ be H_k , H_{k+1} , and H_{k+2} , respectively. Then H_i can be expressed as:

$$H_i = H_k + \frac{i-k}{k+1-k}(H_{k+1} - H_k) + \frac{(i-k)(i-k-1)}{(k+1-k)(k+2-k)}(H_{k+2} - 2H_{k+1} + H_k) \quad (3)$$

For spline interpolation, a series of low-order polynomials are used to fit the data points, each valid within a small interval. For example, in cubic spline interpolation, let the estimated channel response on subcarrier i be H_i , and the spline interpolation coefficients calculated based on known channel responses be a , b , c , d . Then H_i can be expressed as:

$$H_i = a + b(i-k) + c(i-k)^2 + d(i-k)^3 \quad (4)$$

However, these traditional interpolation methods may face challenges when dealing with high dynamic ranges or nonlinear channel conditions. Especially in rapidly changing channel environments, these methods may not accurately capture the dynamic characteristics of the channel. Moreover, traditional methods often rely on prior assumptions about channel characteristics, which may not always hold true in practical applications. Therefore, there is a need for more efficient and accurate channel estimation methods.

In recent years, the application of machine learning techniques in channel estimation has attracted widespread attention. These methods can better capture the dynamic changes of the channel by learning its statistical characteristics. Compared to traditional interpolation methods, machine learning-based methods can adaptively handle different channel conditions without relying on strict mathematical models. Therefore, the application of machine learning in interpolation channel estimation offers new possibilities for improving the accuracy and adaptability of the estimation.

2.2 GAN-based Interpolation Channel Estimation

In the field of computer vision, deep learning techniques, especially Generative Adversarial Networks (GANs), have proven their exceptional performance in image generation, denoising, super-resolution, and other areas. Given GANs' capability in simulating complex data distributions, the communication field has also started to widely adopt this machine learning method for channel estimation.

We can consider the Channel Frequency Response (CFR) as a specific format of "image," where the real and imaginary parts of the channel correspond to different channels of the image. This imaging method not only provides an intuitive way to observe and analyze channel characteristics but also enables us to use GANs for channel estimation.

In GAN-based interpolation channel estimation, the task of the generator is to predict the entire channel state based on partially known pilot signals, similar to filling in the blank areas around known pixels in an image. Compared to traditional methods, this learning-based approach can better capture the nonlinear characteristics and dynamic changes of the channel, thus providing a more accurate estimation. The role of the discriminator is to distinguish between the estimated channel generated by the generator and the real channel, thereby guiding the generator to produce more accurate channel estimations. Once the GAN training is completed, we can input the partially known pilot signals into the trained generator to generate the entire channel pilot. The adaptability of this method enables it to adapt to various complex real channel conditions.

However, like traditional interpolation methods, GAN-based interpolation channel estimation also requires a certain number of known signals as input, which somewhat limits its application scope. Furthermore, to achieve optimal performance in GAN-based interpolation channel estimation, a large amount of channel measurement data is typically needed for training to ensure that the GAN can accurately learn and simulate the actual channel characteristics. When dealing with large-scale channel estimation tasks, traditional machine learning methods may face computational resource limitations. Therefore, to overcome these limitations, introducing quantum machine learning for interpolation channel estimation has become an attractive direction. Quantum computing has shown potential advantages in processing large-scale data and high-dimensional problems. Quantum machine learning is expected to provide a more efficient and accurate channel estimation method, thus meeting the growing demand for channel estimation performance in future wireless communication systems.

3. Quantum Computing and Quantum Generative Adversarial Networks

3.1 Basics of Quantum Computing

Quantum computing is a research method exploring the intersection of computer science and quantum physics. Its aim is to discover the potential of quantum systems in information processing. It leverages certain characteristics of quantum mechanics, such as superposition, entanglement, and quantum tunneling effects, to perform computational tasks [22]. While traditional bits in computing can only be 0 or 1, a quantum bit (qubit) can simultaneously be in a superposition state of both 0 and 1 as:

$$|\psi\rangle = \alpha|0\rangle + \beta|1\rangle \quad (5)$$

Where α and β are complex numbers satisfying $|\alpha|^2 + |\beta|^2 = 1$. When measuring a qubit, it collapses to the $|0\rangle$ state with probability $|\alpha|^2$ and to the $|1\rangle$ state with probability $|\beta|^2$. This superposition property allows for parallelism in quantum computing.

Quantum logic gates serve as basic units to operate on qubits. Unlike classical AND, OR, NOT gates, quantum gates preserve the superposition and entanglement properties when acting on qubits. Some commonly used quantum gates include:

$$X = \begin{bmatrix} 0 & 1 \\ 1 & 0 \end{bmatrix} \quad Y = \begin{bmatrix} 0 & -i \\ i & 0 \end{bmatrix} \quad Z = \begin{bmatrix} 1 & 0 \\ 0 & -1 \end{bmatrix} \quad H = \frac{1}{\sqrt{2}} \begin{bmatrix} 1 & 1 \\ 1 & -1 \end{bmatrix} \quad CNOT = \begin{bmatrix} 1 & 0 & 0 & 0 \\ 0 & 1 & 0 & 0 \\ 0 & 0 & 0 & 1 \\ 0 & 0 & 1 & 0 \end{bmatrix} \quad (6)$$

The Pauli X gate, also known as the quantum *NOT* gate, flips states $|0\rangle$ and $|1\rangle$. The Pauli Y gate is a combination of Pauli X and Z gates, introducing a complex number i . The Pauli Z gate introduces a negative phase for the $|1\rangle$ state. The Hadamard gate (H) is often used to create superposition states; applying H to $|0\rangle$ or $|1\rangle$ transforms it into a superposition state. The CNOT gate is a two-qubit gate; if the control qubit is in $|1\rangle$, the target qubit is flipped, otherwise, it remains unchanged. Here's an example of creating an entangled state:

Suppose we have two qubits, starting at $|00\rangle$. Applying H gate to the first qubit, we get:

$$(H \otimes I)|00\rangle = \frac{1}{\sqrt{2}}(|0\rangle + |1\rangle) \otimes |0\rangle = \frac{1}{\sqrt{2}}(|00\rangle + |10\rangle) \quad (7)$$

Applying the CNOT gate to this superposition state with the first qubit as the control and the second as the target, we get an entangled state:

$$CNOT\left(\frac{1}{\sqrt{2}}(|00\rangle + |10\rangle)\right) = \frac{1}{\sqrt{2}}(|00\rangle + |11\rangle) \quad (8)$$

If one of the qubits is measured, the state of the other qubit will also be instantly determined, regardless of the distance between them. This is the magic of quantum entanglement.

3.2 Variational Quantum Circuits (VQC)

Variational Quantum Circuits (VQC) are central components of quantum-classical hybrid algorithms. They function similarly to classical neural networks. The main idea of VQC is to design a parameterized quantum circuit and use classical optimization algorithms to find the optimal values of these parameters to solve a specific problem [20].

The parameterized quantum circuit starts from a ground state (usually all qubits in $|0\rangle$) and passes it through a parameterized quantum circuit composed of rotation and controlled gates. These gate operations are controlled by a set of parameters $\theta = \{\theta_1, \theta_2, \dots, \theta_n\}$. The overall process is described by:

$$U(\theta)|0\rangle^{\otimes n} = |\psi(\theta)\rangle \quad (9)$$

Where $U(\theta)$ is the parameterized quantum circuit and $|\psi(\theta)\rangle$ is the output quantum state.

To solve optimization problems, a cost function $C(\theta)$ is typically defined. In many optimization problems, this cost function is represented as the inner product of the solution vector with a given cost matrix. Assuming a cost matrix H (describing the problem to be optimized), the goal is to find a state $|s\rangle$ such that $\langle s|H|s\rangle$ is minimized. However, in the variational quantum algorithm, one aims to find a set of parameters θ that minimize $\langle \psi(\theta)|H|\psi(\theta)\rangle$, hence the VQC cost function is defined as:

$$C(\theta) = \langle \psi(\theta)|H|\psi(\theta)\rangle \quad (10)$$

To find parameters θ that minimize $C(\theta)$, classical optimization algorithms like gradient descent or quantum natural gradient are used. In each iteration, the cost function $C(\theta)$ is computed for the current θ , and then classical optimization algorithms are used to update the parameters θ accordingly.

3.3 Quantum Generative Adversarial Networks (QGANs)

QGAN (Quantum Generative Adversarial Network) is a Generative Adversarial Network based on quantum computers [23]. It is designed to generate new data that is similar to a real dataset. The purpose of QGAN is to leverage the advantages of quantum computing to provide better performance or faster training speeds on certain specific tasks.

Fundamentally, QGAN operates on principles similar to classical GANs, but the specific implementation is executed on quantum computers through a trainable parameterized quantum circuit. **Fig. 2** shows the architecture of the Quantum Generative Adversarial Network: The QGAN starts with a random quantum state (usually a superposition state of one or more qubits) as noise input to the quantum generator G [15]; The quantum generator G then employs a series of quantum gates (e.g., Pauli X, Y, Z rotations and CNOT gates, etc.) to transform the initial state. The selection and sequence of these quantum gates define a quantum circuit, and the parameters within each gate (e.g., angles of rotation) are what we aim to optimize through training; Next, the state produced by the generator or the quantum state corresponding to real data is input into the quantum discriminator D , which is also a quantum circuit. It processes the input quantum state through a series of quantum operations and then measures the final quantum state, outputting a number between 0 and 1. This number indicates the probability that it perceives the input data as genuine (in practical applications, the discriminator might measure the same input state multiple times and compute the average to mitigate the noise and errors inherent in quantum computations); Both the performances of quantum generator G and quantum discriminator D are then assessed via a loss function, and optimization algorithms such as gradient descent update their parameters. In conventional GANs, the generator aims to maximize the discriminator's error in misjudging its synthetic data as real, while the discriminator's goal is to minimize the misjudgment rate for both real and fake data. This objective remains consistent in QGANs. However, since both the generator and discriminator are quantum circuits, optimization algorithms tailored for quantum circuits, like the quantum version of gradient descent, are employed; Throughout each iteration, both the quantum generator G and quantum discriminator D endeavor to enhance their performances: G tries to produce increasingly realistic data, while D aims to differentiate between generated and real data more accurately. This iterative process continues until the parameters of G and D (rotation angles in the quantum gates) stabilize or reach a predetermined maximum number of iterations.

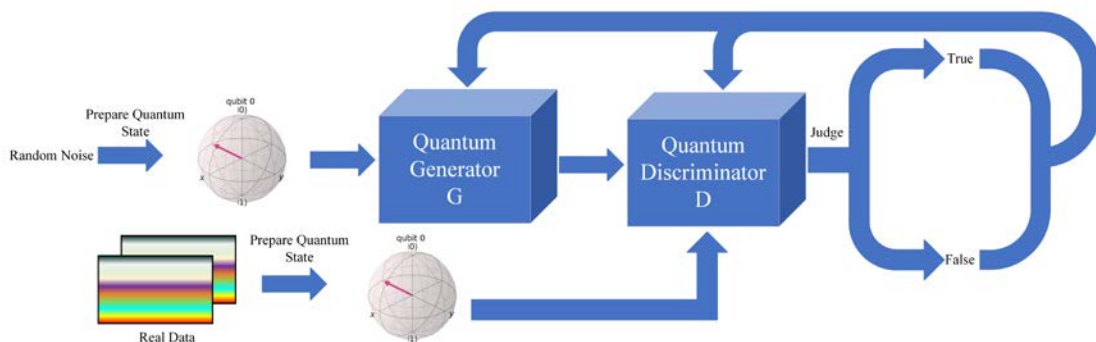


Fig. 2. Quantum generative adversarial network architecture

4. Channel Estimation Based on Dual-Module QGAN

4.1 Network Model of Dual-Module QGAN

The traditional single-module Quantum Generative Adversarial Network (QGAN) might overemphasize the overall characteristics of the data, specifically, the statistical channel features, when generating data similar to the real ones. This bias could result in generated data displaying an average or "generic" trait, thereby overlooking the rich diversity and transient

channel characteristics inherent in real data. To address this issue, we propose a dual-module QGAN design. As depicted in Fig. 3, the two network modules of the quantum generator respectively focus on the holistic and individual characteristics of the data. Specifically, the goal of the first module is to optimize the discriminator's accuracy, ensuring the overall accuracy of the generated data. In contrast, the second module is dedicated to minimizing the mean square error between the generated and real data, ensuring preservation of the data's transient properties.

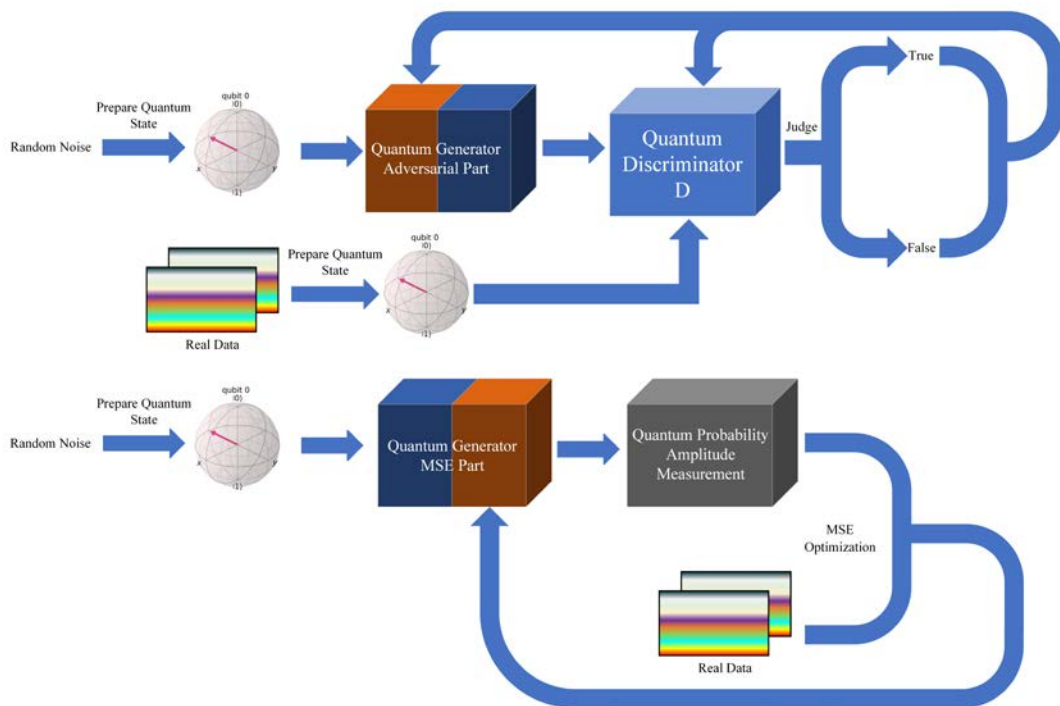


Fig. 3. Dual module generator quantum generation adversarial network architecture

While the dual-module design theoretically offers a more comprehensive optimization mechanism, it also introduces challenges. Firstly, there might be potential objective conflicts between the two modules. For instance, if the first module excessively optimizes the statistical channel features, it may compromise the second module's effort to retain the data's transient properties. Therefore, to ensure the harmonious collaboration of both modules, balancing and reconciling their relationships are crucial. Additionally, compared to the single-module design, the dual-module QGAN introduces added complexity, which might elevate computational burden and training time.

In summary, the dual-module QGAN provides a more flexible and robust framework for channel estimation. By meticulously designing and balancing the relationship between the two modules, we aspire to capture the statistical and transient characteristics of the channel more accurately, thereby enhancing channel estimation performance.

4.2 Quantum Encoding of Channel Information

Quantum amplitude encoding is a method to encode classical data into quantum bits[20]. Its core idea is to encode individual elements of a classical vector as the amplitudes of a quantum

state. This allows us to represent a classical vector using fewer quantum bits. Let's define a normalized classical vector \vec{a} , with elements $\{a_0, a_1, \dots, a_{n-1}\}$, where $n = 2^N$ (N is the number of quantum bits). This vector is encoded into an N -qubit quantum state $|\psi\rangle$, which can be expressed as:

$$|\psi\rangle = \sum_{n=0}^{2^N-1} a_n |i\rangle \tag{11}$$

Where $|i\rangle$ is the computational basis state, which can be $|00\dots 0\rangle, |00\dots 1\rangle, \dots, |11\dots 1\rangle$.

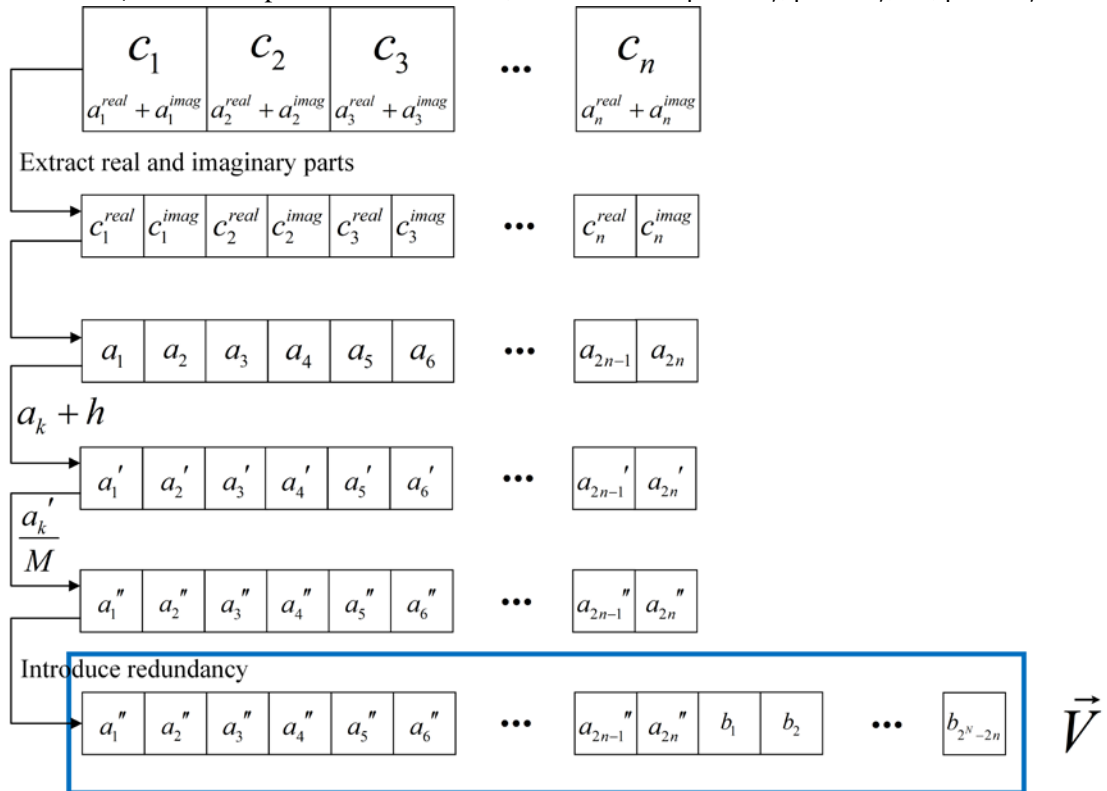


Fig. 4. Pretreatment process of channel pilot information

The pretreatment process for channel pilot information before inputting it into a quantum circuit is illustrated in **Fig. 4**. Let $C = \{c_1, c_2, \dots, c_n\}$ be a set containing n complex numbers, where each complex number c_i corresponds to the channel pilot information. To map these n channel pilot information onto N qubits (where $2^N > 2n$), we first extract the real and imaginary parts from each complex number c_i , resulting in $2n$ real numbers forming the data vector $\vec{A} = \{a_1, a_2, \dots, a_k, \dots, a_{2n}\} = \{c_1^{real}, c_1^{imag}, c_2^{real}, c_2^{imag}, \dots, c_n^{real}, c_n^{imag}\}$.

To ensure the non-negativity required for amplitude encoding, add a preset positive constant h to each real number a_k in the data vector \vec{A} :

$$a'_k = a_k + h \quad \text{for } k = 1, 2, \dots, 2n \tag{12}$$

To meet the amplitude normalization condition, introduce a normalization coefficient M and adjust the first $2n$ elements:

$$a_k'' = \frac{a_k'}{M} \quad \text{for } k = 1, 2, \dots, 2n \quad (13)$$

The square sum of a_k'' is denoted as S :

$$S = \sum_{k=1}^{2n} (a_k'')^2 \quad (14)$$

Subsequently, the square sum of the redundant parameters R is defined as:

$$R = 1 - S \quad (15)$$

Each redundant parameter b_l is:

$$b_l = \sqrt{\frac{R}{2^N - 2n}} \quad \text{for } l = 1, 2, \dots, 2^N - 2n \quad (16)$$

In summary, the complete normalized vector is:

$$\vec{V} = \{a_1'', a_2'', \dots, a_k'', \dots, a_{2n}'', b_1, b_2, \dots, b_l, \dots, b_{2^N - 2n}\} \quad (17)$$

Vector \vec{V} meets the normalization condition of the quantum system, i.e., the sum of squares of its elements is 1 and can be used for quantum amplitude encoding.

When a certain probability amplitude v_i' is measured from the quantum state, the denormalization process for each element \vec{V}' is:

$$a_n''' = M \times v_i' - k \quad \text{for } i = 1, 2, \dots, 2^N \quad (18)$$

Thus, after removing the redundancy, the obtained vector corresponds to the original channel pilot information.

4.3 Quantum Generator and Quantum Discriminator Network Structure

In our research, we adopted a method based on parameterized quantum circuits to design the quantum generator and quantum discriminator[15]. As shown in Figure Fig. 5, this structure mainly involves single qubit rotations around the X and Z axes. By adjusting the rotation angles, this structure can perform a variety of single qubit transformations. Additionally, by incorporating ZZ rotations, the structure successfully introduces quantum entanglement, a key quantum mechanism that allows for rich interactions between qubits. Such entanglement not only enhances the circuit's representational power but also enables it to precisely describe complex data distributions.

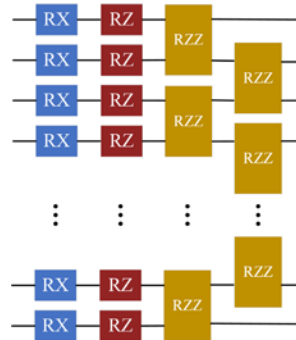


Fig. 5. Basic layer of quantum generator and quantum discriminator

Considering the potential limitations in representational power of a single-layer structure, we used a multi-layer stacking strategy to more effectively approximate and represent various complex quantum states. When this basic layer structure is repeated numerous times, approaching an infinite number of layers, it achieves universality in quantum computation. This means, theoretically, it can generate or discriminate any quantum state.

It's worth noting that since this structure uses simple quantum gates based on the Pauli operators, these gates can easily be implemented on current quantum hardware. This not only ensures its theoretical soundness but also means it has a high feasibility on actual quantum computing hardware.

In conclusion, the basic layer structure designed for the generator and discriminator has demonstrated its superiority and powerful capability in practice. It successfully merges the universality of quantum circuits, the flexibility of single-qubit gate transformations, the entanglement properties brought by two-qubit gates, and adaptability to real hardware, providing a solid theoretical and practical foundation for the development of Quantum Generative Adversarial Networks (QGANs).

The QGAN network designed in this paper can be implemented on real quantum computers. However, as current real quantum computer technology is still in the NISQ (Noisy Intermediate-Scale Quantum) era, issues like stability, scalability, especially noise and decoherence, limit the capability to conduct large-scale and high-precision experiments. Under these circumstances, simulating quantum computer operations on classical computers becomes a viable strategy, providing us with a theoretical framework to simulate, understand, and optimize the QGAN training process, even if it can't capture all the nuances of quantum hardware. The detailed structure of the quantum generator and discriminator is shown in **Fig. 6.**

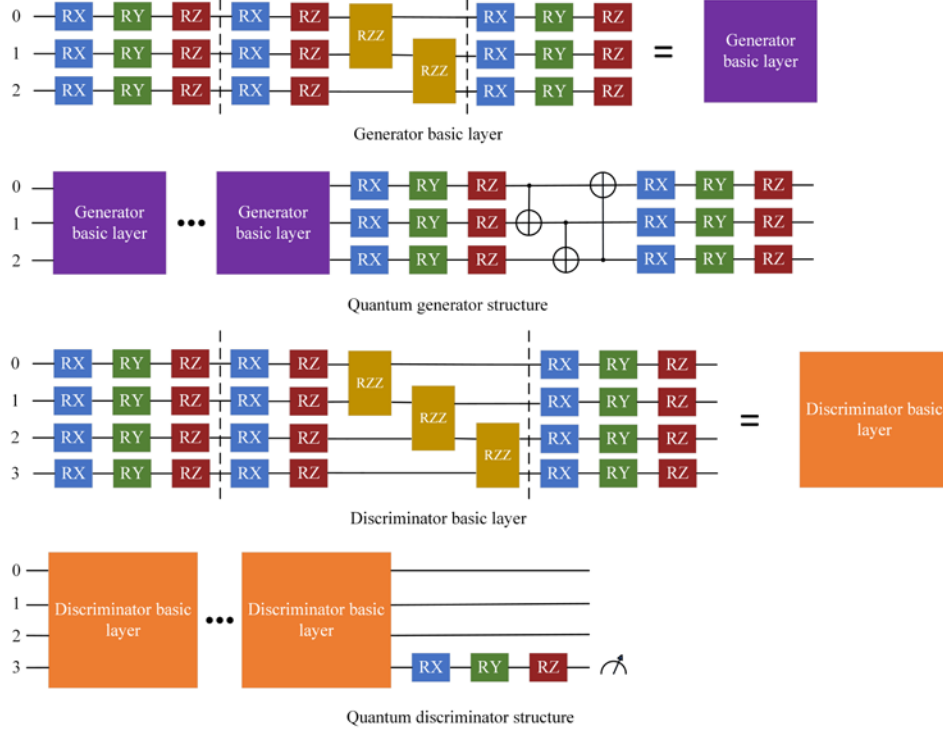


Fig. 6. Structure of quantum generator and quantum discriminator

In a typical quantum computing setup, certain qubits are used for data loading, while others play specific roles, such as serving as the output of the quantum discriminator. The measurement of this output qubit is essentially making a specific observation, often related to the Pauli-Z operator, to measure its expectation value.

Let our qubit be in the state $|\psi\rangle$, and our measurement operator be the Pauli-Z operator M . Then the expected measurement value is:

$$\langle M \rangle = \langle \psi | M | \psi \rangle \quad (19)$$

Where $\langle \psi | M | \psi \rangle$ describes the expected value obtained when measuring a specific quantum state.

The expected value of the measurement lies between $[-1,1]$. To map this value to a probability range of $[0,1]$, we use the following simple linear transformation:

$$P = \frac{\langle M \rangle + 1}{2} \quad (20)$$

In this way, P represents the probability that the discriminator believes the input is real data. A probability close to 1 means the discriminator is more confident that the input is real, while a value closer to 0 indicates it believes the input was generated by the generator.

4.4 Channel Estimation Algorithm Based on Dual-Module QGAN

QGANs, through adversarial training strategies, enable the generator to gradually learn and simulate the statistical distribution of real channel data. However, a notable drawback of this

method is that it often overlooks the characteristics of instantaneous channel information, leading to certain limitations in real-time applications.

On the other hand, Mean Squared Error (MSE) optimization is a method widely used in machine learning and signal processing. Its main advantage lies in ensuring that the generated data is as numerically close as possible to the real data, providing convenience for real-time processing. However, relying solely on MSE optimization may lose the ability to capture higher-level statistical characteristics, and thus relying solely on MSE may result in poor generalization performance of the network.

Considering the advantages and disadvantages of the above two methods, we propose a combined strategy aimed at fully utilizing the characteristics of QGANs and MSE. Specifically, we decompose the quantum generator into two parts: one part is responsible for adversarial generation to capture complex statistical channel information; the other part focuses on MSE optimization to ensure the numerical accuracy of the generated data. By alternating between the two optimization strategies, we expect the generator to not only effectively capture the statistical characteristics of the channel but also ensure its accuracy in terms of instantaneous characteristics.

To better explore the combined strategy we propose, it is first necessary to emphasize that although the quantum network structure adopted by this strategy is overall similar to traditional quantum generative adversarial networks, we have made specific design adjustments in the part of the quantum generator. Specifically, the quantum generator is subdivided into two specialized parts: the first part focuses on adversarial generation to capture and emulate real data's statistical features; the second part is dedicated to optimizing the Mean Squared Error (MSE) to ensure the numerical closeness of the generated data to the real data. The network structure of the dual-module quantum generator is shown in Fig. 7:

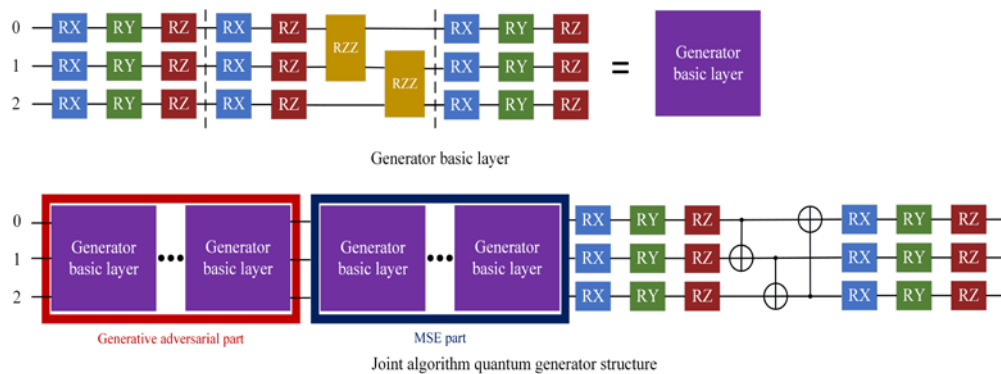


Fig. 7. Structure of joint algorithm quantum generator

Although we have made such design adjustments to the quantum generator, the function and structure of the quantum discriminator remain unchanged. Its main task is still to judge whether the input data is generated by the quantum generator, thereby assisting the generator to optimize better.

In this paper, partial pilot information and noise are used as inputs for the generator, simulating real application scenarios where only partial pilot information is available, and the complete channel information is obtained through the trained quantum generative adversarial network. Such a design not only makes full use of the existing partial channel information but also enhances the model's generalization ability, making it more robust in practical applications.

During the training process, the generator is divided into the adversarial generation part and the mean squared error part. The loss function is defined as follows:

$$cost = \lambda \times loss_g + (1 - \lambda) \times loss_m \quad (21)$$

The goal of this loss function design is twofold: the adversarial generation part aims to deceive the discriminator with the generated data, while the mean squared error part ensures that the generated data is as close as possible to the real data. If relying solely on a single loss function, such as using only the adversarial loss, the model might overly focus on generating data to deceive the discriminator, neglecting the differences from the real data. Conversely, if relying solely on the mean squared error, the model might overly focus on the precise matching of each data point, ignoring the overall distribution of the data. Therefore, by combining both, we can ensure that the model can learn the overall distribution characteristics of the real data and ensure that the point-to-point error between the generated data and the real data is minimized. To achieve this balance, we adjust the weight parameter λ , so that the two parts of the loss complement each other during training, avoiding any one side having an excessive influence on the model training.

The training method of the dual-module quantum generative adversarial network is shown in [Table 1](#):

Table 1. Quantum generative adversarial network joint MSE optimization algorithm

Quantum Generative Adversarial Network Joint MSE Optimization
<p>Inputs: Real channel pilot information dataset: <code>real_data</code> Adversarial part learning rate: lr_{gan} Mean squared error (MSE) part learning rate: lr_{mse} Maximum number of iterations: <code>max_epochs</code> Number of quantum bits: N Amount of pilot information data per set: n Weight of the adversarial part's loss function in the total loss function of the dual-module generator: λ_1 Weight of the MSE part's loss function in the total loss function of the dual-module generator: λ_2</p>
<p>Initialization: 1. Load the real channel pilot information data <code>real_data</code> into the quantum register $\psi_{real}\rangle$</p> <ul style="list-style-type: none"> • Set up a quantum register of size N quantum bits. • After normalizing the data, load it into the register using quantum amplitude encoding. <p>2. Combine partial real pilot information and noise to create the dataset with partial pilot information: <code>fake_data</code>.</p> <p>3. Load the partial pilot information <code>fake_data</code> into the quantum register $\psi_{fake}\rangle$</p> <p>4. Initialize the adversarial parameters of the quantum generator G as θ_{g_gan}</p> <p>5. Initialize the MSE parameters of the quantum generator G as θ_{g_mse}</p> <p>6. Initialize the parameters of the quantum discriminator D as θ_d</p>

For each epoch in range(max_epochs):

For quantum_state $|\psi_{real}\rangle$ in real_data:

- The quantum state $|\psi_{fake}\rangle$ passes through the generator to create a fake full pilot quantum state $|\psi_{fake}'\rangle$.
- Use the discriminator to evaluate real and fake data.
 $real_score = \langle \psi_{real} | D(\theta_d) | \psi_{real} \rangle$
 $fake_score = \langle \psi_{fake}' | D(\theta_d) | \psi_{fake}' \rangle$
- Denormalize the generated quantum state $|\psi_{fake}'\rangle$ to get the corresponding classical data: generate_data.
- Calculate the MSE between the generated data generate_data and real_data.

$$MSE = \frac{1}{n} \sum_{i=1}^n (real_data - generate_data)^2$$

- Calculate adversarial loss and MSE loss.
 $loss_d = -(\log(real_score) + \log(1 - fake_score))$ # Discriminator loss
 $loss_g = -\log(fake_score)$ # Adversarial part loss
 $loss_m = MSE$ # MSE part loss
- Calculate the loss functions $cost_g, cost_m$ for the generator's adversarial part and MSE part, respectively.

$$cost_g = \lambda_1 \times loss_g + (1 - \lambda_1) \times loss_m$$

$$cost_m = \lambda_2 \times loss_g + (1 - \lambda_2) \times loss_m$$

- Update the parameters θ_{g_gan} of the generator G's adversarial part and discriminator D's parameters θ_d .

$$\theta_{g_gan} = \theta_{g_gan} - lr_{gan} * \nabla_{\theta_{g_gan}} cost_g$$

$$\theta_d = \theta_d - lr_{gan} * \nabla_{\theta_d} loss_d$$

- Update the parameters θ_{g_mse} of the generator G's MSE part and the discriminator D's parameters θ_d .

$$\theta_{g_mse} = \theta_{g_mse} - lr_{mse} * \nabla_{\theta_{g_mse}} cost_m$$

$$\theta_d = \theta_d - lr_{mse} * \nabla_{\theta_d} loss_d$$

Output: Optimized generator G and discriminator D.

5. Experimental Simulation and Results Analysis

Given the current technological limitations of real quantum computers, the quantum amplitude encoding module required for this study cannot yet be implemented on real quantum computers with more than two qubits. Therefore, this research utilizes the PennyLane platform to simulate quantum computing operations on classical computers. To generate the training dataset, this study first performs a Fourier transform on multipath Rayleigh fading channels to obtain the frequency domain channel H. Subsequently, the input to the quantum generator is the channel H_p at the pilot points in H, while the comparator channel for the discriminator is the initially generated H. This process aims to simulate the training of the dual-module quantum generative adversarial network in a noise-free environment. After training, this paper

will compare the dual-module quantum generative adversarial network with traditional interpolation channel estimation methods under noisy channel conditions.

Fig. 8 shows the comparison of the mean squared error (MSE) between the real pilot data using a non-dual-module QGAN and the pilot data before and after inputting it into the QGAN as the number of iterations increases. **Fig. 8(a)** displays the MSE between the partial pilot data plus random noise and the complete real pilot data, while **Fig. 8(b)** shows the MSE between the complete pilot data generated after processing by the non-dual-module QGAN and the complete real pilot data. From the comparison of these two figures, it can be seen that the MSE before inputting into the non-dual-module QGAN is generally higher. However, as the number of iterations increases, the pilot data generated by the non-dual-module QGAN, although still exhibiting higher MSE levels at certain moments, shows overall improvement. This indicates that the non-dual-module QGAN has enabled the quantum generator to learn some core features of the data through multiple iterations, but these features mainly target the overall characteristics of the data rather than specific values. In the field of channel estimation, this is not the desired outcome, so using a dual-module QGAN to address the issue of a general QGAN's inability to learn instantaneous channel features is particularly important.

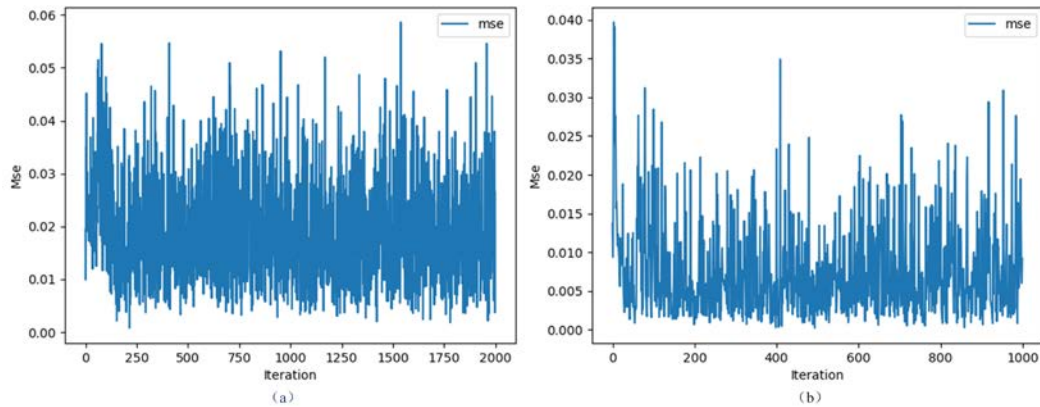


Fig. 8. Comparison of mean square error between (a) input data and real channel pilot data, and (b) generated data and real channel pilot data.

Fig. 9 shows the changes in the performance of the non-dual-module quantum generator and quantum discriminator as the number of iterations increases. **Fig. 9(a)** displays the change in the accuracy of the quantum discriminator's judgments as the number of iterations increases. As training progresses, the discriminator's accuracy in identifying generated data remains around 50%, indicating that the discriminator can no longer clearly distinguish between generated and real data. In identifying real data, its accuracy remains around 75%, suggesting that the discriminator's decisions are based on certain data features rather than being completely random.

Fig. 9(b) shows the changes in the losses of the quantum generator and quantum discriminator as the training progresses. As shown in the figure, as training deepens, $loss_d$ (discriminator loss) and $loss_g$ (generator loss) gradually stabilize. Around 250 iterations, the quantum generator and quantum discriminator reach Nash equilibrium, at which point the training of the quantum generative adversarial network can be considered essentially complete. However, due to the inherent properties of quantum systems, the loss curves exhibit relatively

high volatility.

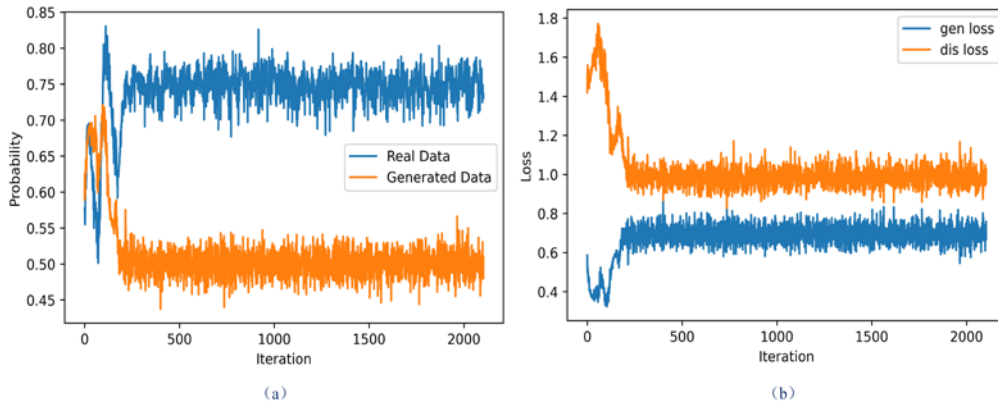


Fig. 9. Performance evolution of quantum generator and discriminator during QGAN training

Fig. 10 shows the change in the accuracy of the quantum discriminator's judgments in the dual-module QGAN as the number of iterations increases. After about 700 iterations, it can be observed that the accuracy of judgments enters a relatively stable phase, indicating that the system is gradually approaching Nash equilibrium. In this state, the probability of the discriminator judging the generated data as real data remains at the 50% level, while the accuracy of identifying real data is slightly higher, at about 56%. It is worth noting that the change curve of the quantum discriminator's judgment accuracy is smoother compared to that of the non-dual-module QGAN. This phenomenon is due to the integration of the Mean Squared Error (MSE) loss into the loss function during the training of the generator, resulting in smoother changes in the generated data. However, this also leads to an increase in the number of iterations required to reach Nash equilibrium.

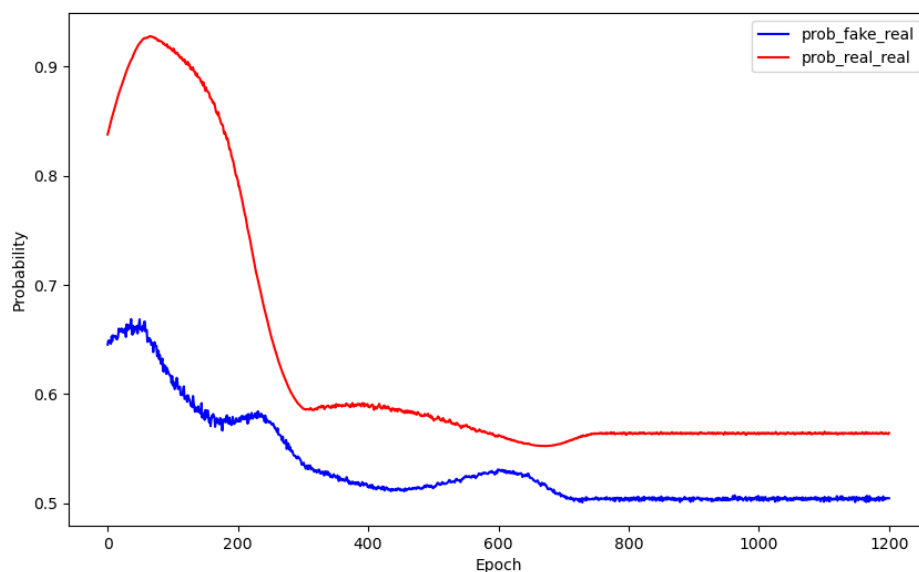


Fig. 10. Changes in the decision accuracy of QGAN optimization combined with MSE

Fig. 11 shows the change in the mean squared error (MSE) between the complete pilot data generated from partial pilot data and the real pilot data in the dual-module QGAN on the training and test sets as the number of training iterations increases. **Fig. 11(a)** shows the changes on the training set, from which it can be observed that the MSE continuously decreases as the number of iterations increases, demonstrating the gradual adaptation and learning of the dual-module quantum generator to the training data. This continuous improvement trend indicates that our optimization strategy has gradually improved the model's accuracy on the training set. However, several fluctuations occurred before reaching Nash equilibrium, due to the presence of "barren plateaus" characterized by exponentially vanishing gradients in deep quantum parametric circuits, cost functions of global observables, and noisy circuits, leading the model to fall into local optima. Although the MSE performance is good at this time, the discriminator does not consider the data generated at this time to have the core features of real data, and further optimization of network parameters is needed.

Fig. 11(b) shows the changes in MSE on the test set. As the number of iterations increases, the MSE between the pilot data generated by the dual-module QGAN and the real pilot data, inputting previously unseen partial pilot information, also decreases. This indicates that the dual-module QGAN has not only learned the overall channel characteristics but also that the generated data is close to the real values, demonstrating that the model has not experienced overfitting and possesses good generalization properties. However, due to falling into local optima during training, the MSE curve on the test set also exhibits fluctuations before training completion.

Considering these two subfigures, we can conclude that through joint mean squared error optimization, the QGAN not only exhibits superior performance during the training phase but also demonstrates excellent robustness and generalization capability during the testing phase.

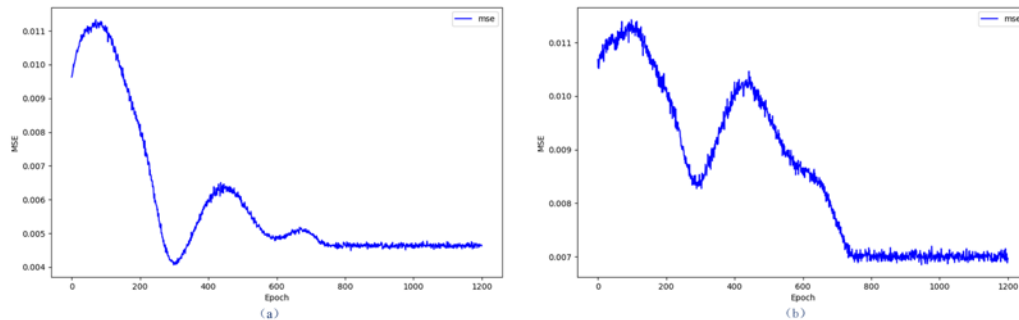


Fig. 11. Error evolution of (a) training set and (b) test set under QGAN combined with MSE optimization

Fig. 12 shows the comparison results between the dual-module QGAN and the classical interpolation channel estimation method under different noise conditions. From the figure, it can be seen that as the noise level increases, the mean squared error (MSE) between the pilot information generated by the classical interpolation channel estimation method and the pilot information of the noise-free channel gradually increases. In contrast, the performance of the dual-module QGAN proposed in this paper is comparable to the classical method at low noise levels (below 5dB), demonstrating good adaptability. However, at high noise levels (above 5dB), the performance of the dual-module QGAN is significantly better than the classical method, with a noticeably lower MSE, indicating stronger robustness in handling high noise channel estimation, thus reflecting the advanced nature of this method. This is attributed to the

dual-module quantum generator having learned the statistical and instantaneous characteristics of the noise-free channel during the training process, enabling it to function like a "pilot transmitter" in practical applications, generating pilot information very close to the real pilot data.

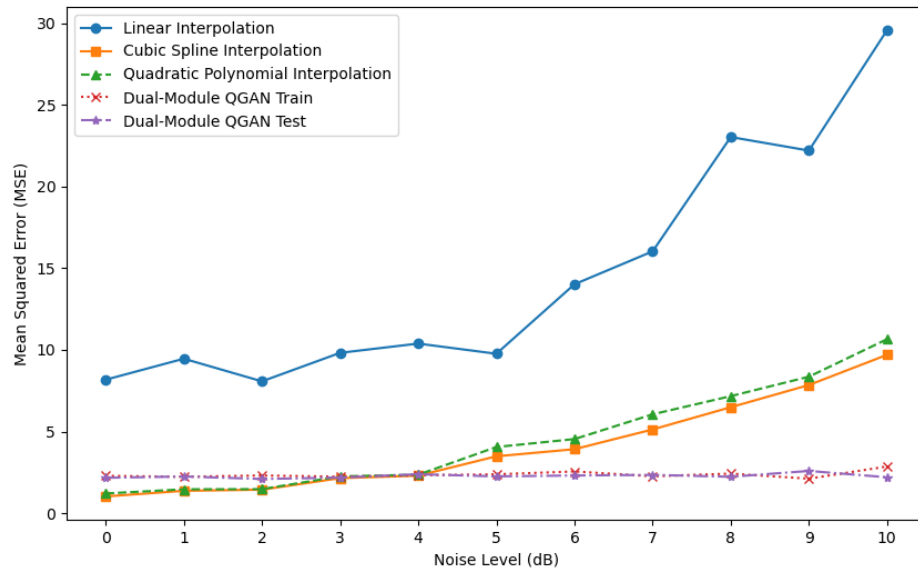


Fig. 12. MSE of Different Channel Estimation Methods with Increasing Noise Levels

6. Conclusion

The quantum generative adversarial network (QGAN) scheme proposed in this paper inherits the powerful capabilities of traditional GANs and introduces the advantages of quantum computing, aiming to provide more accurate and efficient tools for channel estimation. However, relying solely on QGAN still cannot fully solve the problem of precise estimation of instantaneous channel information. Therefore, we further introduce the Mean Squared Error (MSE) optimization strategy to ensure that the generated channel information is as close as possible to the actual situation. Through experimental research, this paper demonstrates the superior performance of QGAN combined with MSE optimization in channel estimation. With the development of quantum computers and the continuous increase in the number of quantum bits, the data scale that can be processed will also grow exponentially, showing more obvious advantages for the high-dimensional and large-scale data processing of future 6G mobile communication. This provides strong theoretical support and practical guidance for the further development of future wireless communication technology, especially in the field of channel estimation. Overall, this study not only proposes a novel and effective channel estimation scheme but also opens a new chapter in the integration of quantum technology and wireless communication, providing new ideas for future wireless communication research and applications.

References

- [1] J. G. Andrews et al., "What will 5G be?," *IEEE J. Sel. Areas Commun.*, vol. 32, no. 6, pp. 1065-1082, 2014. [Article \(CrossRef Link\)](#)
- [2] S. Buzzi et al., "A Survey of Energy-Efficient Techniques for 5G Networks and Challenges Ahead," *IEEE J. Sel. Areas Commun.*, vol. 34, no. 4, pp. 697-709, Apr. 2016. [Article \(CrossRef Link\)](#)
- [3] C. E. Shannon, "A Mathematical Theory of Communication," *Bell Syst. Tech. J.*, vol. 27, no. 3, pp. 379-423, 1948. [Article \(CrossRef Link\)](#)
- [4] R. Hadani et al., "Orthogonal Time Frequency Space Modulation," in *Proc. of IEEE Wireless Commun. Netw. Conf. (WCNC)*, San Francisco, CA, pp. 1-6, 2017. [Article \(CrossRef Link\)](#)
- [5] Z. Wei et al., "Orthogonal Time Frequency Space Modulation: A Promising Next-Generation Waveform," *IEEE Wireless Commun.*, vol. 28, no. 4, pp. 136-144, Aug. 2021. [Article \(CrossRef Link\)](#)
- [6] S. K. Mohammed, "Derivation of OTFS Modulation from First Principles," *IEEE Trans. Veh. Technol.*, vol. 70, no. 8, pp. 7619-7636, Aug. 2021. [Article \(CrossRef Link\)](#)
- [7] M. K. Ramachandran and A. Chockalingam, "MIMO-OTFS in High-Doppler Fading Channels: Signal Detection and Channel Estimation," in *Proc. of IEEE Global Commun. Conf. (GLOBECOM)*, Abu Dhabi, United Arab Emirates, pp. 206-212, 2018. [Article \(CrossRef Link\)](#)
- [8] S. K. Sengupta, "Fundamentals of Statistical Signal Processing: Estimation Theory," *Control Engineering Practice*, vol. 37, no. 4, pp. 465-466, 1994. [Article \(CrossRef Link\)](#)
- [9] H. Ye, G. Y. Li, and B.-H. F. Juang, "Power of Deep Learning for Channel Estimation and Signal Detection in OFDM Systems," *IEEE Wireless Commun. Lett.*, vol. 7, no. 1, pp. 114-117, Feb. 2018. [Article \(CrossRef Link\)](#)
- [10] I. Goodfellow et al., "Generative Adversarial Nets," in *Proc. of Adv. Neural Inf. Process. Syst.*, pp. 2672-2680, 2014. [Article \(CrossRef Link\)](#)
- [11] A. M. Elbir and K. V. Mishra, "Federated Learning for Channel Estimation in Conventional and IRS-Assisted MIMO Systems," *IEEE Commun. Lett.*, vol. 25, no. 7, pp. 2344-2348, July 2021. [Article \(CrossRef Link\)](#)
- [12] X. Ma and Z. Gao, "Data-Driven Deep Learning to Design Pilot and Channel Estimator for Massive MIMO," *IEEE Trans. Veh. Technol.*, vol. 69, no. 5, pp. 5677-5682, May 2020. [Article \(CrossRef Link\)](#)
- [13] A. Taha, Y. Zhang, and F. B. Mismar, "Enabling Large Intelligent Surfaces with Compressive Sensing and Deep Learning," *IEEE Access*, vol. 9, pp. 44304-44321, 2021. [Article \(CrossRef Link\)](#)
- [14] S. B. Amiri et al., "Machine Learning-Enabled LOS/NLOS Identification for MIMO Systems in Dynamic Environments," *IEEE Trans. Cogn. Commun. Netw.*, vol. 7, no. 1, pp. 88-100, Mar. 2021. [Article \(CrossRef Link\)](#)
- [15] S. Lloyd and C. Weedbrook, "Quantum Generative Adversarial Learning," *Phys. Rev. Lett.*, vol. 121, no. 4, July 2018. [Article \(CrossRef Link\)](#)
- [16] H.-L. Huang et al., "Experimental Quantum Generative Adversarial Networks for Image Generation," *Phys. Rev. Appl.*, vol. 16, no. 2, Aug. 2021. [Article \(CrossRef Link\)](#)
- [17] V. Dunjko and H. J. Briegel, "Machine Learning & Artificial Intelligence in the Quantum Domain: A Review of Recent Progress," *Rep. Prog. Phys.*, vol. 81, no. 7, 2017. [Article \(CrossRef Link\)](#)
- [18] A. Abbas et al., "The Power of Quantum Neural Networks," *Nat. Comput. Sci.*, vol. 1, no. 6, pp. 403-409, June 2021. [Article \(CrossRef Link\)](#)
- [19] P.-L. Dallaire-Demers and N. Killoran, "Quantum Generative Adversarial Networks," *Phys. Rev. A*, vol. 98, no. 1, July 2018. [Article \(CrossRef Link\)](#)
- [20] Y. Cao et al., "Quantum Chemistry in the Age of Quantum Computing," *Chem. Rev.*, vol. 119, no. 19, pp. 10856-10915, Oct. 2019. [Article \(CrossRef Link\)](#)
- [21] J. G. Proakis & M. Salehi, *Digital Communications*, 5th Edition, 2008. [Article \(CrossRef Link\)](#)

- [22] M. A. Nielsen & I. L. Chuang, *Quantum Computation and Quantum Information: 10th Anniversary Edition*, Cambridge: Cambridge University Press, 2010. [Article \(CrossRef Link\)](#)
- [23] G. Verdon, J. Pye, & M. Broughton, "A Universal Training Algorithm for Quantum Deep Learning," 2018. [Article \(CrossRef Link\)](#)



Ting Li received the B.S., M.S. and Ph.D. degrees from School of information Science and Engineering, Southeast University, Nanjing, China, in 2001, 2004, and 2009, respectively. He is currently an associate professor at the College of Communication and Information Engineering, Nanjing University of Posts and Telecommunications, China. He has published more than 40 research papers. His research interests include wireless communication for 6G, quantum computing, and quantum machine learning.



Zhang Jinbiao was born in 1997 in Yangzhou, Jiangsu Province, China. He obtained bachelor's degree in 2019 from the School of Communication and Information Engineering at Yanshan University, Hebei, China. Currently, he is pursuing a master's degree at the School of Communication and Information Engineering, Nanjing University of Posts and Telecommunications, China. His research focuses on quantum machine learning